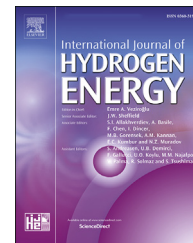


Available online at www.sciencedirect.com

ScienceDirect

journal homepage: www.elsevier.com/locate/he

Online adaptive water management fault diagnosis of PEMFC based on orthogonal linear discriminant analysis and relevance vector machine

Shangwei Zhou ^{a,*}, Jaspreet Singh Dhupia ^b^a School of Automotive Studies, Tongji University, No. 4800 Cao'an Road, Shanghai 201804, PR China^b Department of Mechanical Engineering, University of Auckland, Auckland 1010, New Zealand

HIGHLIGHTS

- An online adaptive strategy based on posterior probability of RVM is proposed.
- Orthogonal linear discriminant analysis was employed as feature extraction method.
- Single cell voltages are considered as the original diagnostic variables.
- The diagnostic accuracy can be maintained when the characteristic of system changed.

ARTICLE INFO

Article history:

Received 25 August 2019

Received in revised form

23 December 2019

Accepted 27 December 2019

Available online xxx

Keywords:

Proton exchange membrane fuel cell (PEMFC)

Orthogonal linear discriminant analysis (OLDA)

Relevance vector machine (RVM)

Water management failure

Online adaptive diagnostics

ABSTRACT

A data-driven strategy for characterizing the water management failure in a Proton Exchange Membrane Fuel Cell (PEMFC) is presented in this paper. To carry out the diagnosis of water management failure, first the original single cell voltages are projected into lower-dimension features by applying orthogonal linear discriminant analysis (OLDA). Then, a classification methodology termed relevance vector machine (RVM) is employed to classify the lower-dimension features into different categories that indicate the respective health states of the system. The initially trained projecting vectors and classifiers lose their efficiency gradually the characteristics of PEMFC system change, such as the cell voltages decaying with time due to the normal degradation due to aging. An online adaptive diagnostic strategy based on the posterior probability of RVM is proposed, so as to keep the diagnostic accuracy over time. The efficiency and reliability of this online adaptive diagnostic strategy is validated using an experimental database from a 90-cell PEMFC stack.

© 2020 Hydrogen Energy Publications LLC. Published by Elsevier Ltd. All rights reserved.

Introduction

There is a mounting interest in the research and development of the Proton Exchange Membrane Fuel Cell (PEMFC) technology because of several desirable characteristics such as

high efficiency, high-power density, lowering carbon footprint and its ability to operate at low temperature (generally 60–80 °C) [1–3]. Thus, it is predicted that PEMFC can become an alternative power converter for automobile, stationary and portable applications in near future [4].

* Corresponding author.

E-mail address: shangw.zhou@gmail.com (S. Zhou).

<https://doi.org/10.1016/j.ijhydene.2019.12.193>

0360-3199/© 2020 Hydrogen Energy Publications LLC. Published by Elsevier Ltd. All rights reserved.

However, the water management in a PEMFC is a critical barrier to be surmounted to ensure its satisfactory performance and durability. The main water transportation and balance mechanisms across the membrane electrolyte assembly (MEA) incorporate electro-osmotic drag, back diffusion, hydraulic permeation and thermal-osmotic drag [5]. It is challenging to attain a subtle water equilibrium, where enough water is provided for maintaining the efficient ionic conductivity of the membrane, while avoiding excess water droplets which hinders the transportation of the reactants. An insufficient level of humidification causes an increase in the ohmic losses and can result in an irreversible membrane damage [6,7]. Excessive water droplets accumulated in the flow channels, gas diffusion layers (GDL) and catalyst layers (CL) obstructs the arrival rate of reactants which also results in a reduction of performance [8–10]. To improve the water management, from the perspective of stack design and development, a hydrophilic water transport plate is employed as the bipolar plate in Ref. [11], adding hydrophilic SiO₂ particles to the anode CL is proposed in Ref. [12] and innovative design of flow channels is proposed in Ref. [13] respectively. Besides, a timely diagnosis of the water management failure can adjust the control commands to avert a possible degradation and extend the system's lifespan. For example, Ref. [14] presented a Fault Tolerant Control Strategy (FTCS) for remedial adjusting of the inlet air flow rate, which was based on the diagnosis models to let the stack recover from a flooding failure.

Several diagnostic approaches have been developed, each with its own advantages and weaknesses. These approaches include physical models-based [15–17], electrochemical impedance spectroscopy (EIS) [18–21] and nonlinear frequency response analysis [22]. The model-based diagnosis is usually carried out in two stages: generation and evaluation of the residual. The residual is generated from the difference between the model estimations and the actual measurements. The emergence of a fault is presumed when the residual exceeds a preset threshold. An accurate and complete parameters identification is required for such methods and it is difficult to be implemented online due to the high computational effort [23]. On the other hand, the impedance spectra methods like EIS carry out a non-destructive characterization of the electrochemical process dynamics. In EIS, a small amplitude perturbation (voltage or current) at variable frequency is imposed to system during its steady-state operation [24]. However, the perturbation input may disturb normal running of the PEMFC system, besides, the equipment of the EIS is too expensive for in situ usage.

Other approaches have also been proposed, for instance, those using statistical methodology [25], signal-based approaches like analyzing electrochemical noise [26,27], empirical mode decomposition of stack output voltage [28], multifractal spectrum [29], and those using novel micro sensors [30]. However, drawbacks of these approaches include high computational costs and extra equipment.

Instead, the data-driven approaches, such as artificial techniques and statistical techniques, which do not need theoretical relations of physical process and implement fast, are well suitable for PEMFCs complex nonlinear system. Neural networks were used as a fault diagnosis tool for PEMFC in Refs. [31–34], and demonstrated to deliver a high diagnostic rate and generalization ability. Liu et al. [35] presented a novel failure diagnostic approach that was based on extreme

learning machine (ELM) algorithm and Dempster-Shafer (D-S) theory. Using this approach several different levels of excess air stoichiometry failures can be recognized with low computational cost and the approach was able to identify faults in an incipient stage. In Ref. [36], Fisher discrimination analysis (FDA) is adopted to project the original 20-dimension single cell voltages to a lower-dimensional feature. Gaussian mixture model (GMM) was used as a classification methodology, which resulted in low error rates for the diagnostic results and small computational cost, thus the method shown to be suitable for online application. Support vector machine (SVM) methodology was employed for accomplishing the fault detection and identification in Refs. [37–40]. Mao et al. [41] compared the performance of feature selection using kernel FDA and kernel principle component analysis (PCA), and showed that different states (normal or faulty) of original datasets can be separated by a supervised kernel FDA. An overview and comparison of the different non-model based methodologies was presented in Ref. [42].

The previous online diagnosis procedure is usually implemented in two stages [37]. First, during the offline training stage a fixed classifier is acquired based on the experimental database and prior information. Then, during the subsequent online diagnosis, the real-time measurements (e.g. cell voltages) are identified by the fixed classifier to ascertain whether and which faults arise. Nevertheless, the fixed classifier trained using the historical database cannot be used effectively with the PEMFC system for a long-term operation. This is because of the initial fixed classifier losing its efficiency as the characteristics of the PEMFC system change over time, such as the cell voltages gradually decreasing as a consequence of the ageing decay effect (with the agglomeration of Pt catalytic particles). To alleviate such degradation of performance for the PEMFC system, a methodology for selecting features independent of degradation in EIS measurement was presented in Ref. [43].

In view of the aforementioned limitations, the objective of this study is to propose an online adaptive PEMFC fault diagnosis strategy. For one of the common water management faults: the flooding, single cell voltages are selected to serve as the original diagnostic variables. Orthogonal linear discriminant analysis (OLDA) and relevance vector machine (RVM) are used for the feature extraction and classification algorithm, respectively. Furthermore, an online adaptive strategy is proposed to update the projecting vector and RVM classifier in real-time. The performance and the technical feasibility of the online adaptive strategy are evaluated based on the experimental database from a 90-cell PEMFC stack. The dynamic updating is realized by the proposed online adaptive strategy, along with the change of PEMFC system characteristics, which demonstrated the capacity of the proposed strategy to carry out the diagnosis with high accuracy and reliability.

The rest of this paper is organized as follows. Section [Diagnosis algorithms](#) introduces the diagnostic methodologies. Section [Online adaptive strategy](#) details the online adaptive diagnosis strategy. The realization of the proposed strategy and results are presented in Section [Implementation and results from the proposed adaptive diagnosis strategy](#). This section also compares and discuss the performance between the fixed and the adaptive classifier. Finally, Section [Conclusion](#) concludes this work.

Diagnosis algorithms

The principle of orthogonal linear discriminant analysis

The original data set in the high-dimensional space often contains redundancy (linear dependence) and noise. Therefore, using it directly results in errors, a reduction in the classification algorithm accuracy, and an increase of the calculations cost. Thus, the feature extraction is a vital step in the data pre-

The OLDA algorithm defines the following matrices.

$$\begin{aligned} \mathbf{H}_w &= [\mathbf{V}_1 - \mathbf{m}_1 \mathbf{e}_1^T, \dots, \mathbf{V}_c - \mathbf{m}_c \mathbf{e}_c^T] \in \mathbb{R}^{d \times N} \\ \mathbf{H}_b &= [\sqrt{N_1}(\mathbf{m}_1 - \mathbf{m}), \dots, \sqrt{N_c}(\mathbf{m}_c - \mathbf{m})] \in \mathbb{R}^{d \times c} \end{aligned} \quad (2)$$

$$\mathbf{H}_t = \mathbf{V} - \mathbf{m} \mathbf{e}^T = [\mathbf{v}_1 - \mathbf{m}, \mathbf{v}_2 - \mathbf{m}, \dots, \mathbf{v}_N - \mathbf{m}] \in \mathbb{R}^{d \times N}$$

where $\mathbf{m}_i = (1/N_i) \mathbf{V}_i \mathbf{e}_i$ is the mean of the i -th class, with $\mathbf{e}_i = (1, 1, \dots, 1)^T \in \mathbb{R}^{N_i}$, and the global centroid can be calculated as $\mathbf{m} = (1/N) \mathbf{V} \mathbf{e}$ with $\mathbf{e} = (1, 1, \dots, 1)^T \in \mathbb{R}^N$.

Algorithm 1. OLDA

- 1 Form the matrices \mathbf{H}_w , \mathbf{H}_b and \mathbf{H}_t as in Eq. (2);
- 2 Compute reduced SVD of \mathbf{H}_t as $\mathbf{H}_t = \mathbf{U}_1 \Sigma_1 \mathbf{V}_1^T$;
- 3 $\mathbf{B} \leftarrow \Sigma_1^{-1} \mathbf{U}_1^T \mathbf{H}_b$;
- 4 Compute SVD of \mathbf{B} as $\mathbf{B} = \mathbf{P} \Sigma \mathbf{Q}^T$;
- 5 $\mathbf{X}_q \leftarrow \mathbf{U}_1 \Sigma_1^{-1} \mathbf{P}$;
- 6 Compute QR decomposition of \mathbf{X}_q as $\mathbf{X}_q = \tilde{\mathbf{Q}} \tilde{\mathbf{R}}$;
- 7 $\mathbf{G} \leftarrow \tilde{\mathbf{Q}}$.

processing. In case of a typical PEMFC vehicle, to satisfy the high power demands, the stack is composed of hundreds of single cells in series [44]. Therefore, while the single cell voltages are adopted as the original diagnostic variables, the computational complexity needs to be reduced through a feature extraction process. Consider a data matrix $\mathbf{V} = \{\mathbf{v}_1, \mathbf{v}_2, \dots, \mathbf{v}_N\} \in \mathbb{R}^{d \times N}$, distributed in c classes denoted by $\mathbf{V}_1, \mathbf{V}_2, \dots, \mathbf{V}_c$, where $\mathbf{V}_i \in \mathbb{R}^{d \times N_i}$ consists of N_i training samples from the i -th class which satisfies $\sum_{i=1}^c N_i = N$. The feature extraction step computes the transformation vectors $\mathbf{G} \in \mathbb{R}^{d \times l}$ that projects the original high-dimensional data set onto a lower-dimensional space.

$$\mathbf{G} : \mathbf{v}_i \in \mathbb{R}^d \rightarrow \mathbf{x}_i = \mathbf{G}^T \mathbf{v}_i \in \mathbb{R}^l (l < d) \quad (1)$$

The principle component analysis (PCA) algorithm, does not use the information label class of the given data. Therefore, the PCA directions cannot guarantee the maximal separation of between-class data [45]. However, the linear discriminant analysis (LDA) methodology aims at maximizing the between-class data separation and minimizing the within-class separation. To achieve this objective, the LDA method defines within-class and between-class matrices. Different feature extraction (dimension reduction) and classification algorithms with different combination were applied on a 20-cell PEMFC system to deal with water-related faults in Ref. [46]. The error rate using LDA to extract features was observed to be normally lower than those employing an unsupervised PCA methodology, implying that LDA is more suitable for such fault diagnosis. However, the dimensionality of LDA methodology is strictly upper-bounded by $c - 1$ [47]. Furthermore, the LDA algorithm is ineffective when the within-class scatter matrix is singular. Thus, the orthogonal LDA (OLDA), was proposed as an extension of the classical LDA by Ye et al. [48].

The principle of relevance vector machine

Introduced by Tripping [49], relevance vector machine (RVM) is supervised learning method based on the Bayesian principle, which yields a posterior probabilistic prediction for each class. The performance of SVM and RVM were comparatively investigated upon an increasing numbers of training samples in Ref. [50]. While, both the training time and the number of support vectors increased for SVM, they fluctuated only slightly for RVM. The fewer support/relevance vectors resulted in a decrease in the calculation cost of the decision function for RVM, indicating that this method is more suitable for the online implementation. The superior capacity of RVM compared to SVM for diagnostics is also demonstrated in Refs. [51,52].

Assume that an input-targets training dataset is given as $\{\mathbf{x}_i, t_i\}_{i=1}^N$, where N is the number of samples. The standard RVM [53] with the purpose of inferring the parameter of a mapping $y(\mathbf{x}; \mathbf{w})$ is stated as

$$y(\mathbf{x}; \mathbf{w}) = \sum_{i=1}^N w_i k(\mathbf{x}, \mathbf{x}_i) + w_0 = \mathbf{w}^T \mathbf{K} \quad (3)$$

where $\mathbf{w} = [w_0, w_1, \dots, w_N]^T$ is weight vector, \mathbf{x} is the input vector, and $\mathbf{K} = [k(\mathbf{x}, \mathbf{x}_1), \dots, k(\mathbf{x}, \mathbf{x}_N)]^T$ is a $(N+1) \times N$ design matrix. For two-class classification, the logistic sigmoid function $\sigma(y) = 1/(1+e^{-y})$ is usually applied to $y(\mathbf{x}; \mathbf{w})$. Thus, the posterior probability for the first class C_1 can be expressed as

$$p(t=1|\mathbf{x}) = \sigma[y(\mathbf{x}; \mathbf{w})] \quad (4)$$

Similarly for the second class C_2 ,

$$p(t=0|\mathbf{x}) = 1 - \sigma[y(\mathbf{x}; \mathbf{w})] \quad (5)$$

Presuming the independence of target \mathbf{t} , adopting the Bernoulli distribution, the likelihood function $p(\mathbf{t}|\mathbf{w})$ is

$$P(\mathbf{t}|\mathbf{w}) = \prod_{i=1}^N \{\sigma[y(\mathbf{x}_i; \mathbf{w})]\}^{t_i} \{1 - \sigma[y(\mathbf{x}_i; \mathbf{w})]\}^{1-t_i} \quad (6)$$

The weight \mathbf{w} cannot be obtained analytically, so an approximation procedure is used. Since $p(\mathbf{w}|\mathbf{t}, \alpha) \propto P(\mathbf{t}|\mathbf{w})p(\mathbf{w}|\alpha)$, for a constant α , the maximum *a posteriori* (MAP) estimation of the weight \mathbf{w}_{WAP} , can be acquired by maximizing $P(\mathbf{t}|\mathbf{w})p(\mathbf{w}|\alpha)$.

$$\log[P(\mathbf{t}|\mathbf{w})p(\mathbf{w}|\alpha)] = \sum_{i=1}^N [t_i \log y_i + (1 - t_i) \log(1 - y_i)] - \frac{1}{2} \mathbf{w}^T \mathbf{A} \mathbf{w} \quad (7)$$

where $y_i = \sigma[y(\mathbf{x}_i; \mathbf{w})]$, $\mathbf{A} = \text{diag}(\alpha_0, \alpha_1, \dots, \alpha_N)$. Equation (7) is differentiated twice with respect to \mathbf{w} , yielding the Hessian matrix

$$\nabla_{\mathbf{w}} \nabla_{\mathbf{w}} \log p(\mathbf{w}|\mathbf{t}, \alpha) | \mathbf{w}_{MAP} = -(\Phi^T \mathbf{B} \Phi + \mathbf{A}) \quad (8)$$

where $\mathbf{B} = \text{diag}(\beta_1, \beta_2, \dots, \beta_N)$ and $\beta_i = \sigma[y(\mathbf{x}_i)]\{1 - \sigma[y(\mathbf{x}_i)]\}$.

The hyperparameters in matrix \mathbf{A} are updated using

$$\alpha^{new} = \frac{1 - \alpha_i \Sigma_{ii}}{\mathbf{w}_{MAP}^2} \quad (9)$$

where Σ_{ii} is the i -th diagonal element of the covariance matrix $\Sigma = (\Phi^T \mathbf{B} \Phi + \mathbf{A})^{-1}$, and $\mathbf{w}_{WAP} = \Sigma \Phi^T \mathbf{B} \mathbf{t}$.

Online adaptive strategy

As the PEMFC system is operated over its lifespan, the characteristics of the system change, e.g. the stack voltages exhibit a gradual degradation after a period of running time [54]. Therefore, as illustrated in Fig. 1 the classifier needs to adaptively adjust, otherwise, the fixed classifier applied to the dynamic system will cause errors to creep in the fault detection. Thus, the projecting vectors (feature extraction) and classifier

of the offline training need to be updated online. In an offline training process, the single cell voltages data set and the corresponding class labels are required. However, the class label of the normal operation and the flooding fault is an *a priori* information, which can be obtained through experiments. Online adaptive fault diagnosis also requires the single cell voltages data set and class information as the previous training process. While the former can be collected by real-time sampling, but the corresponding class information cannot be obtained. Furthermore, it is not feasible to carry out experiments at regular intervals over a PEMFC system life-span, and it can adversely affect the system life.

To maintain the efficiency of the diagnosis approach during the long-term operation of a PEMFC system, specific diagnostic rules and an incremental learning methodology spherical shaped multi-class SVM were used for both new fault mode and ageing effects in Refs. [55,56]. It was demonstrated that the performance of the diagnostic approach was maintained, however, an extra diagnosis rule, called new cluster judge was added, which results in an increase in the computation effort online. However, this new cluster rule may lose efficacy, when the arising of a new fault causes the characteristics of the PEMFC system to only change subtly.

The proposed strategy of online adaptive diagnosis based on the posterior probability consists of the offline training, online diagnosis and adaptive updating, as illustrated in Fig. 2. In the offline training process, feature extraction and RVM classification model training are performed on the cell voltage monitor (CVM) data set obtained from the experiment (including normal and faulty operations), from which the projecting vectors and the RVM classifier are obtained. During the online diagnosis stage, first the offline training matrix and the RVM classifier are used to recognize the real-time cell voltage according to the diagnosis rule from the classifier. Also, the posterior probability is obtained at the same time. The adaptive updating process performs real-time sampling according to a preset sampling period T . If the sampling frequency is f , the number of adaptively updated data sets \mathcal{D}_1 is T/f . Since there may be errors in the results from the online diagnostic process, screening is performed based on the

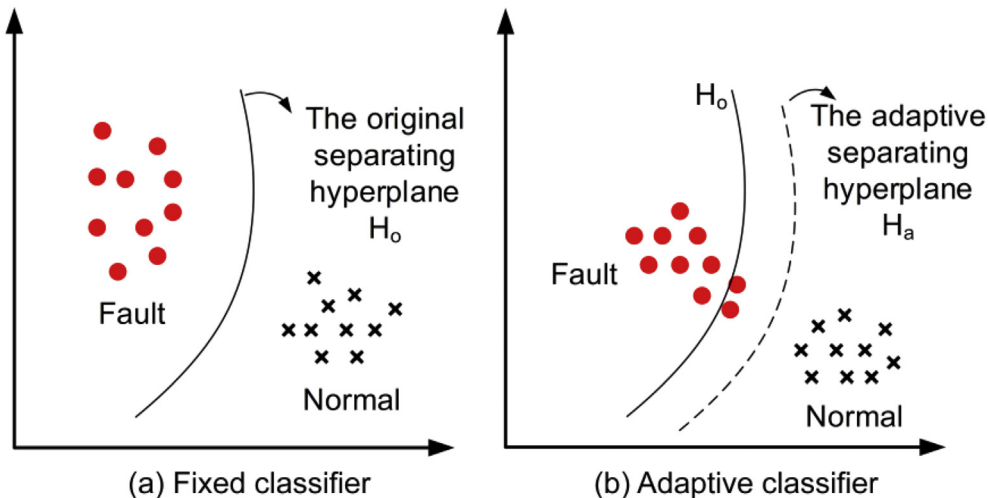


Fig. 1 – Schematic representing fixed classifier and adaptive classifier separating data for normal and faulty operation.

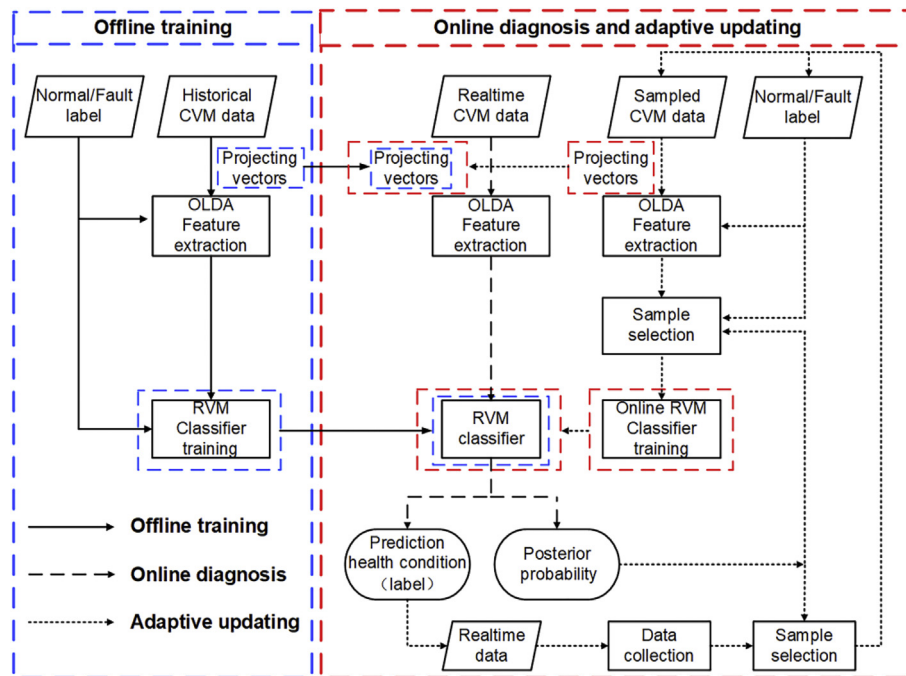


Fig. 2 – The proposed strategy for the online adaptive diagnosis based on posterior probability.

posterior probability for each sample. Misclassified samples, whose posterior probability is below a certain threshold are screened out to avoid an accumulation of the errors. However, when a real-time cell voltage sample is predicted to be normal by the online diagnostic classifier, and the normal posterior probability is greater than the threshold, the data sample is retained as a training sample for the next online sequence.

After data screening, the posterior probability-based data set \mathcal{D}_2 (including normal and faulty case) constructed in the adaptive updating process is then subjected to feature extraction and RVM classification model training which is synchronized with the online diagnosis process. However, unlike the offline training, the reduced-dimensional data can be further screened by the posterior probability to reduce the classifier training samples and the online calculation cost. Due to the sparsity of the RVM algorithm, only a small number of training data set \mathcal{D}_3 can be obtained from a suitable classification performance. After the training is completed, the new projecting vectors and the adaptive RVM classifier are used to refresh the online diagnosis process of the previous cycle.

Implementation and results from the proposed adaptive diagnosis strategy

Experimental setup

The experiments were conducted for the normal and anode flooding condition for a PEMFC stack test bench. The layout of the set up used for investigation is shown in Fig. 3. The main components of the test rig include PEMFC stack, air supply subsystem, hydrogen supply subsystem, coolant subsystem, electronic load and control/supervision unit.

The hydrogen fuel (99.9% H_2 concentration) from a storage tank is regulated by a proportional control valve mixed with recirculation unused anode exhaust, which is continuously supplied to the fuel cell anode inlet. The anode recirculation can increase the hydrogen utilization rate but also humidify the fuel without an extra humidifier. Before the recirculation blower, the anode exhaust gas was also passed through a water knockout, where condensed vapor forms liquid water which is collected and intermittently drained through a valve, which is followed by the removal of the impurities along with a nitrogen purge valve to prevent fuel starvation. At the cathode side, the compressed and electrochemically filtered air is cooled and humidified before feeding into the stack.

The nominal operating conditions of the 90-cell PEMFC stack with an active area of 285 cm^2 used for this investigation are summarized in Table 1.

The experiment is conducted by running the system for 20 min to reach steady-state conditions, and then collecting single cell voltage for 7.5 min under normal condition and 7.5 min under flooding condition. The normal and flooding conditions are created by adjusting the drainage lapse to 40 s and 70 s respectively, where the normal operation drainage lapse of 40 s was determined by experimental calibration. An increase in drainage lapse causes the appearance and accumulation of liquid water on the anode side. The operation time of 7.5 min is also chosen to avoid an irreversible degradation of the fuel cell stack during the flooding condition due to local hydrogen starvation. The extra protective measure of shutting down the system if any of cell voltage fell below zero was also added. The onboard fuel cell controller used a time step of 100 ms. Therefore, based on the computation costs and diagnostic considerations, the sampling frequency of single voltage data was kept at 10 Hz.

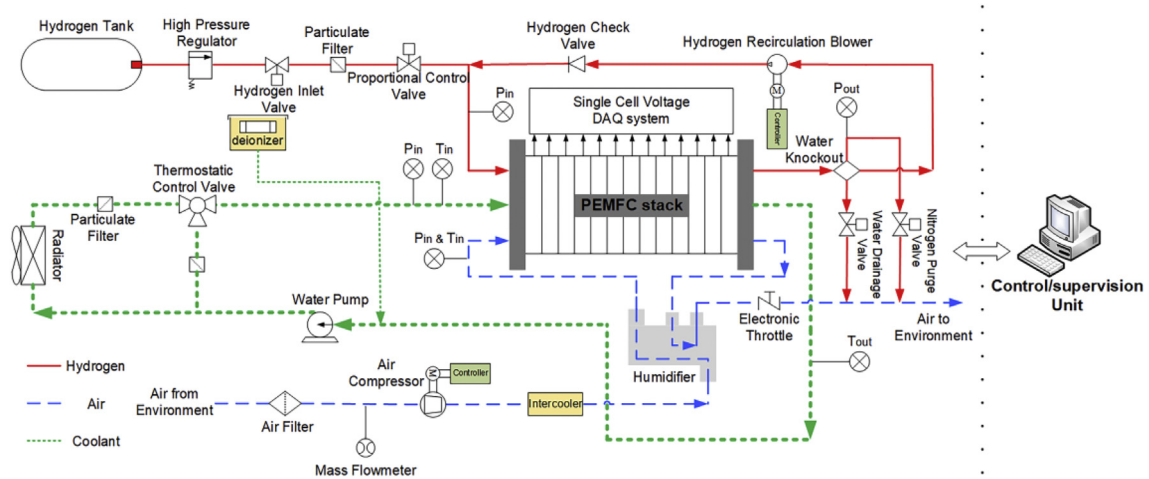


Fig. 3 – Experiment setup for the PEMFC stack.

Table 1 – The nominal operating conditions of the PEMFC stack.

| Stack Parameter | Nominal Value |
|----------------------------|---------------|
| Current | 300A |
| Relative humidity (Air) | 95% |
| Pressure (hydrogen) | 220 kPa |
| Pressure (Air) | 200 kPa |
| Stoichiometry (hydrogen) | 1.6 |
| Stoichiometry (Air) | 1.8 |
| Coolant inlet temperature | 60 °C |
| Coolant outlet temperature | 70 °C |

To perform the online diagnosis, the relationship between the input variables and the output class needs to be established first. Using the OLDA feature extraction training process, the original 90-dimensional single cell voltages were projected to a 5-dimensional feature space followed by the classification step, in which the RVM classifier was trained. Since the 5-dimensional feature space is still difficult to visualize in printed material, two-dimensional images are used for presenting the diagnosis results from fixed and adaptive classifier later. The experimental single cell voltages for training and test are shown in Figs. 4 and 5 respectively.

To validate the effectiveness of the proposed strategy, the test data set $v_1, v_2, \dots, v_n \in \mathbb{R}^M$, $M = 90$ covering normal and flooding fault operations of the stack, which are also presented in Fig. 5, are divided into 21 sequences of online data set each having a time span of 20 s. The test data were labelled in advance (label information is not used in OLDA and RVM online training stage). After that, the trained feature extraction projecting vectors and classifier were employed to process the online test data set. Simultaneously, the diagnostic accuracy of this method was acquired by comparing the classifier predictions with the labelled classes.

Based on the offline training fixed classifier in Fig. 2, which could be regarded as the diagnostic initiation, the 21 online data set sequences are diagnosed in sequential manner.

Classification results based on the fixed classifier

First of all, the performance of the fixed classifier was investigated, where the diagnostic accuracy of the 21 online data set sequences were assessed. The fixed classifier indicates that the separating hyperplane (decision function) of the 21 online data sequences is the same, and the results for some sequence (as numbered within each plot) are presented in Fig. 6.

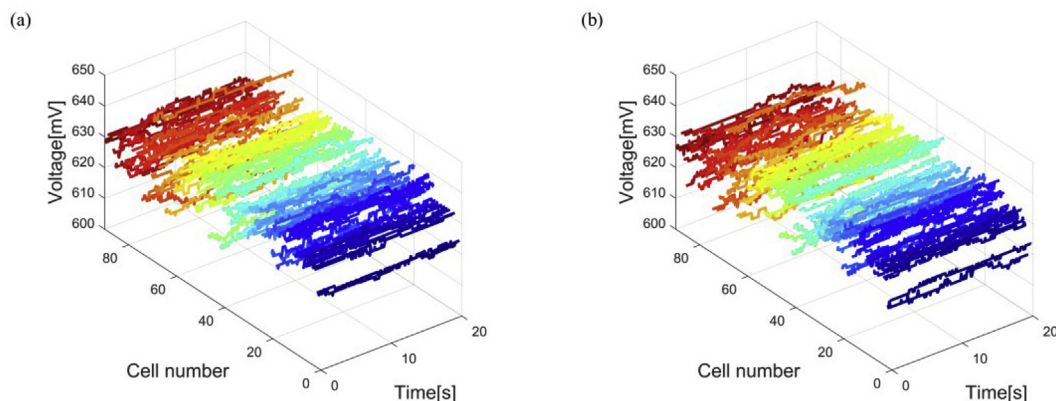


Fig. 4 – Single cell voltages for (a) normal, and (b) flooding states during offline training.

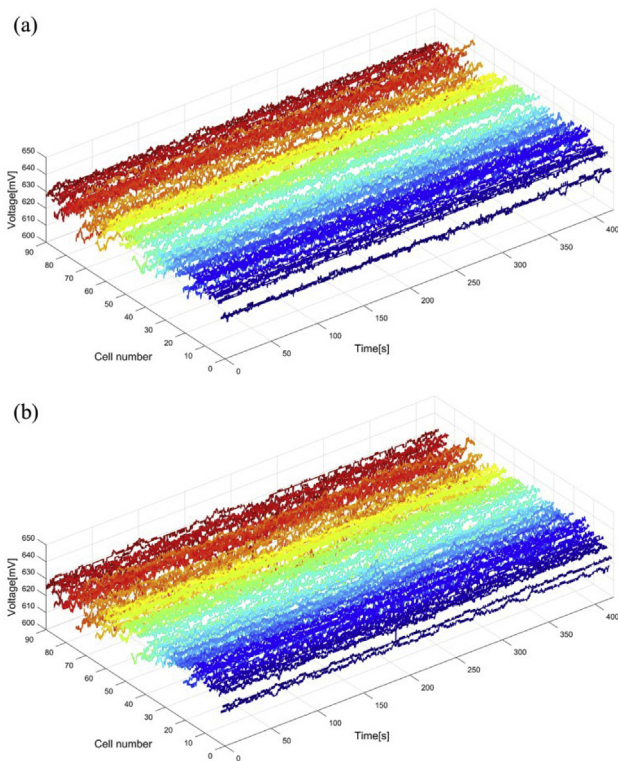


Fig. 5 – Single cell voltages for (a) normal, and (b) flooding states during testing stage.

The average diagnostic accuracy of the OLDA + RVM fixed classifier obtained was 93.3%, and the minimum diagnostic accuracy was 76.3%. Compared with the initial accuracy of 99.8%, the average diagnostic accuracy of the fixed classifier reduced by 6.5%, and the minimum diagnostic accuracy dropped by 23.5% over the 21 online data sets. While the

average diagnostic accuracy of the first ten online data sequences was 99.0%, that for the last eleven online data sequences was 88.2%. Thus, the reliability and efficiency of the fixed classifier was significantly decreased. This observed degradation in diagnostic performance is due to the changes in the system characteristics, which makes the separating hyperplane of the fixed classifier and the original feature extraction matrix inapplicable to the later cell voltage samples.

Classification results based on the online adaptive classifier

Fig. 7 presents the separating hyperplane (position) of the adaptive classifier based on the posterior probability, which can be observed to be dynamically adjusted as the operating state of the system changes. Therefore, the adaptive fault diagnosis strategy implements a dynamic update that avoids misclassifying the data during the PEMFC operation. Although the online diagnosis of 1st and 13th sequences contained a few false predictions, as highlighted in the figure, the data screening based on the posterior probability threshold ($=0.985$) was able to eliminate the misclassified samples, and no propagation of the classification error occurred.

The average diagnostic accuracy of online adaptive OLDA + RVM dynamic classifier based on posterior probability was 99.7%, and the lowest diagnostic accuracy was 95.5%. Compared to the fixed classifier, the average diagnostic accuracy rate has increased by 6.4%, and the minimum diagnostic accuracy rate has increased by 19.2%. The average diagnostic accuracy of the first ten online data sequences is 99.95%, and the last eleven online data sequences is 99.5%. This shows that the online adaptive dynamic classifier based on posterior probability is continuously updated according to the new samples. The misclassification samples are also effectively eliminated, which results in a higher fault

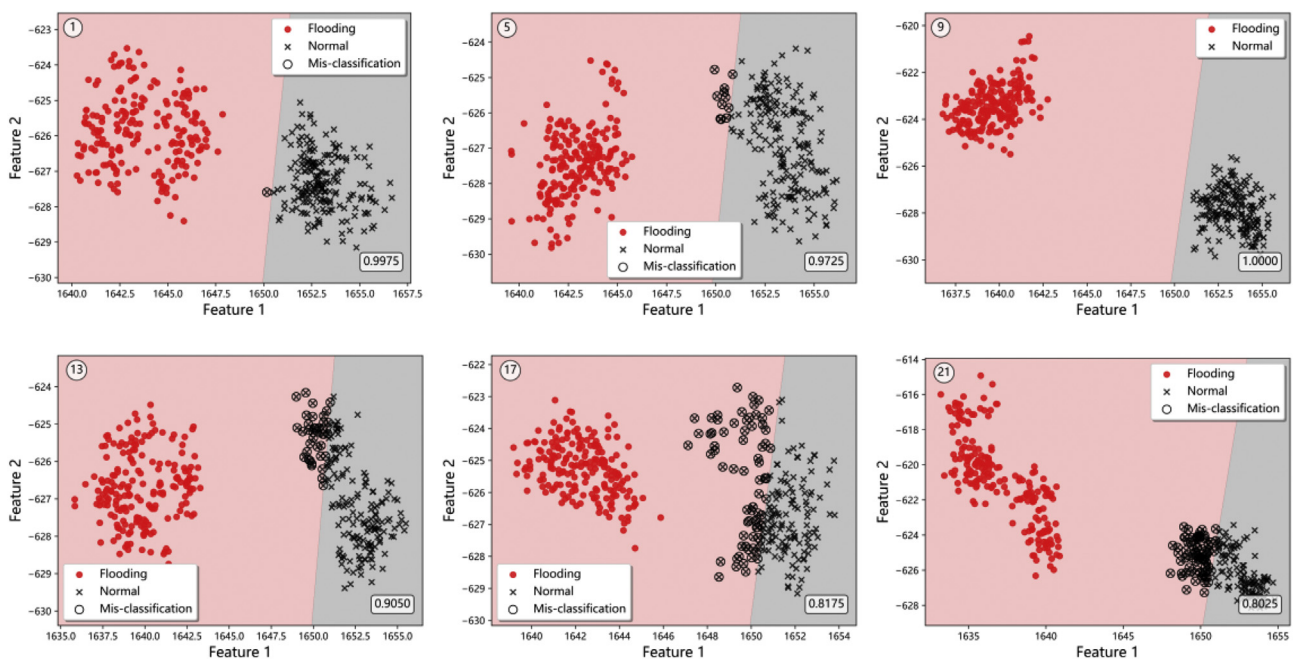


Fig. 6 – Online data sequence diagnosis results of OLDA + RVM fixed classifier.

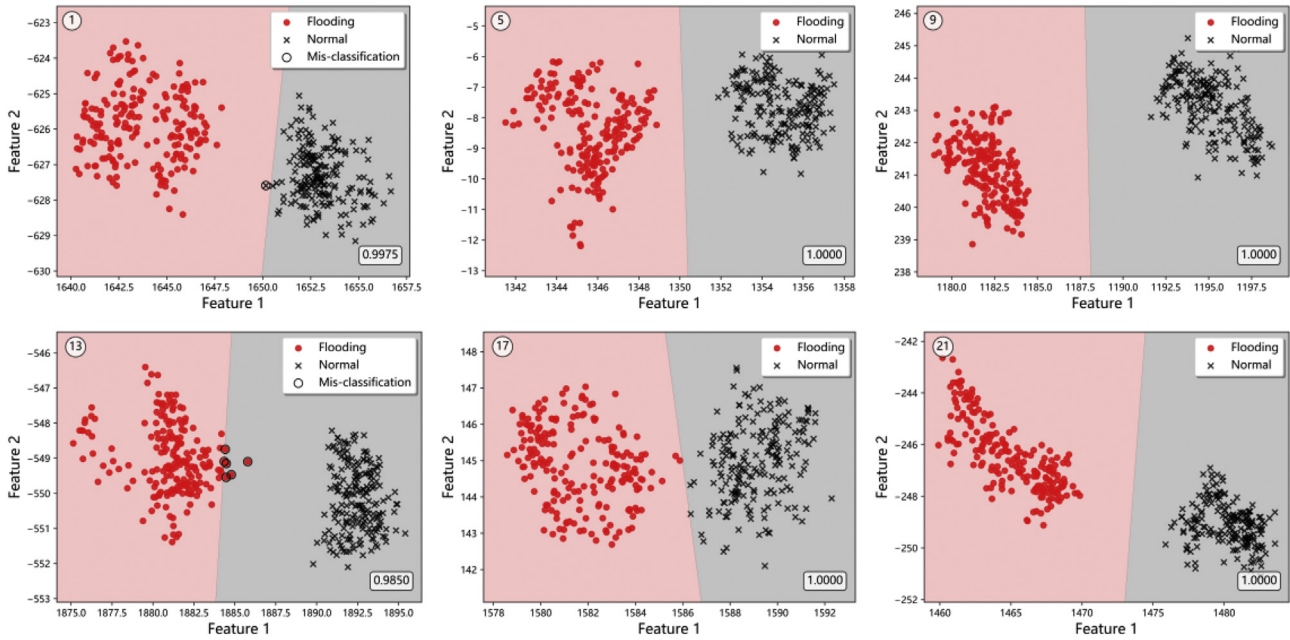


Fig. 7 – Online data sequence diagnosis results of OLDA + RVM adaptive classifier.

diagnosis accuracy rate even when the fuel cell state changes (e.g. in case of the ageing decay effect).

The comparison of the diagnostic performance from different classifiers is shown in Fig. 8. Under practical operating conditions for a PEMFC, where the running time is longer and the fuel cell states can change significantly, the online adaptive dynamic classifier based on the posterior probability will have a better real-time diagnosis performance than the fixed classifier.

In this work, the tests were carried out with a 2.6-GHz CPU and 16-GB RAM programmed with Python 3.7. For this configuration, the adaptive updating process required 0.039s on an average for feature extraction and 1.046 s for RVM classification. The total training time (1.085 s) was much lower than the cycle time (20s) of the online diagnostic process.

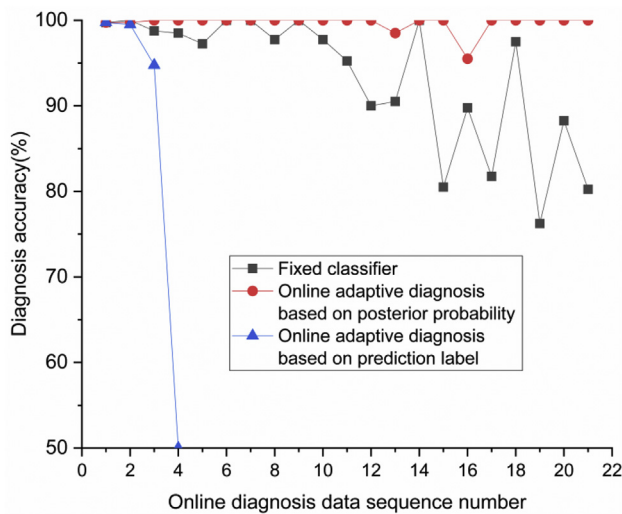


Fig. 8 – Comparison of performance from different diagnosis strategies.

Therefore, the computational costs of the proposed adaptive diagnostic strategy for PEMFC stacks can be considered low enough for the online application.

Conclusions

An online adaptive data-driven strategy is proposed for determining the health states of a PEMFC system in this study. The OLDA methodology, which was able to capture information of all data classes by improving on the upper-bounded limitation of the LDA approach, is adopted in this work for feature extraction, and the sparse RVM is applied to classify the features into the corresponding classes. This method has an advantage of fewer relevance vectors and therefore, lower computational costs, which makes it suitable for online diagnosis with a low complexity.

This proposed approach was experimentally validated on measurements of single cell voltages from a 90-cell PEMFC system operated under normal and flooding fault conditions. The results showed that the proposed approach can identify the flooding fault with a high accuracy. Using an online adaptive strategy according to the posterior probability of RVM output, the projecting vectors and classifier were adapted accordingly over the running time, meanwhile, the misclassified samples are eliminated and thus there was no propagation accumulation of the classification error. Compared to the fixed classifier, the average diagnostic accuracy rate has increased by 6.4%. The minimum diagnostic accuracy rate over the entire running duration increased by 19.2%. Thus, the diagnostic performance was maintained at a satisfactory level throughout the running duration. The next step in this research is to include disturbance within the system dynamics in order to enhance the robustness of the proposed approach.

REFERENCES

- [1] Guo YF, Chen HC, Wang FC. The development of a hybrid PEMFC power system. *Int J Hydrogen Energy* 2015;40:4630–40. <https://doi.org/10.1016/j.ijhydene.2015.01.169>.
- [2] Yogesha S, Brahmabhatt S, Raja M, Arikapudi S, Bhut B, Jaikumar V. Development of hydrogen fuel cell bus technology for urban transport in India. *SAE Technical Paper*; 2019. <https://doi.org/10.4271/2019-26-0092>.
- [3] Jensen H-CB, Schaltz E, Koustrup PS, Andreasen SJ, Kær SK. Evaluation of fuel-cell range extender impact on hybrid electrical vehicle performance. *IEEE Trans Veh Technol* 2012;62:50–60. <https://doi.org/10.1109/TVT.2012.2218840>.
- [4] Yun W, Chen KS, Mishler J, Cho SC, Adroher XC. A review of polymer electrolyte membrane fuel cells: technology, applications, and needs on fundamental research. *Appl Energy* 2011;88:981–1007. <https://doi.org/10.1016/j.apenergy.2010.09.030>.
- [5] Wei D, Wang H, Yuan X-Z, Martin JJ, Yang D, Qiao J, et al. A review on water balance in the membrane electrode assembly of proton exchange membrane fuel cells. *Int J Hydrogen Energy* 2009;34:9461–78. <https://doi.org/10.1016/j.ijhydene.2009.09.017>.
- [6] Chun JH, Park KT, Jo DH, Lee JY, Kim SG, Lee ES, et al. Determination of the pore size distribution of micro porous layer in PEMFC using pore forming agents under various drying conditions. *Int J Hydrogen Energy* 2010;35:11148–53. <https://doi.org/10.1016/j.ijhydene.2010.07.056>.
- [7] Sanchez D, Garcia-Ybarra P. PEMFC operation failure under severe dehydration. *Int J Hydrogen Energy* 2012;37:7279–88. <https://doi.org/10.1016/j.ijhydene.2011.11.059>.
- [8] Lin G, Van Nguyen T. Effect of thickness and hydrophobic polymer content of the gas diffusion layer on electrode flooding level in a PEMFC. *J Electrochem Soc* 2005;152:A1942–8. <https://doi.org/10.1149/1.2006487>.
- [9] Ito K, Ashikaga K, Masuda H, Oshima T, Kakimoto Y, Sasaki K. Estimation of flooding in PEMFC gas diffusion layer by differential pressure measurement. *J Power Sources* 2008;175:732–8. <https://doi.org/10.1016/j.jpowsour.2007.10.019>.
- [10] Shimpalee S, Beuscher U, Zee JWV. Analysis of GDL flooding effects on PEMFC performance. *Electrochim Acta* 2007;52(24):6748–54. <https://doi.org/10.1016/j.electacta.2007.04.115>.
- [11] Wang Z, Zeng Y, Sun S, Shao Z, Yi B. Improvement of PEMFC water management by employing water transport plate as bipolar plate. *Int J Hydrogen Energy* 2017;42:21922–9. <https://doi.org/10.1016/j.ijhydene.2017.07.052>.
- [12] Jung UH, Jeong SU, Park KT, Lee HM, Chun K, Choi DW, et al. Improvement of water management in air-breathing and air-blowing PEMFC at low temperature using hydrophilic silica nano-particles. *Int J Hydrogen Energy* 2007;32:4459–65. <https://doi.org/10.1016/j.ijhydene.2007.05.008>.
- [13] Bunmark N, Limtrakul S, Fowler MW, Vatanatham T, Gostick J. Assisted water management in a PEMFC with a modified flow field and its effect on performance. *Int J Hydrogen Energy* 2010;35:6887–96. <https://doi.org/10.1016/j.ijhydene.2010.04.027>.
- [14] Lebreton C, Benne M, Damour C, et al. Fault Tolerant control strategy applied to PEMFC water management. *Int J Hydrogen Energy* 2015;40:10636–46. <https://doi.org/10.1016/j.ijhydene.2015.06.115>.
- [15] Escobet T, Feroldi D, Lira Sd, Puig V, Quevedo J, Riera J, et al. Model-based fault diagnosis in PEM fuel cell systems. *J Power Sources* 2009;192:216–23. <https://doi.org/10.1016/j.jpowsour.2008.12.014>.
- [16] Polverino P, Frisk E, Jung D, Krysanter M, Pianese C. Model-based diagnosis through structural analysis and causal computation for automotive polymer electrolyte membrane fuel cell systems. *J Power Sources* 2018;357:26–40. <https://doi.org/10.1016/j.jpowsour.2017.04.089>.
- [17] Lira SD, Puig V, Quevedo J. Robust LPV model-based sensor fault diagnosis and estimation for a PEM fuel cell system. In: 2010 conference on control and fault-tolerant systems (SysTol). IEEE; 2010. p. 819–24. <https://doi.org/10.1109/SYSTOL.2010.5676000>.
- [18] Yuan X, Sun JC, Blanco M, Wang H, Zhang J, Wilkinson DP. AC impedance diagnosis of a 500 W PEM fuel cell stack: Part I: stack impedance. *J Power Sources* 2006;161:920–8. <https://doi.org/10.1016/j.jpowsour.2006.05.003>.
- [19] Rodat S, Sailler S, Druart F, Thivel P-X, Bultel Y, Ozil P. EIS measurements in the diagnosis of the environment within a PEMFC stack. *J Appl Electrochem* 2010;40:911–20. <https://doi.org/10.1007/s10800-009-9969-0>.
- [20] NAKAJIMA Hironori, KONOMI Toshiaki, KITAHARA Tatsumi, et al. Electrochemical impedance parameters for the diagnosis of a polymer electrolyte fuel cell poisoned by carbon monoxide in reformed hydrogen fuel. *Transactions of the Asme Journal of Fuel Cell Science & Technology* 2008;5:129–33. <https://doi.org/10.1115/1.2931462>.
- [21] Tant S, Rosini S, Thivel P-X, Druart F, Rakotondrainibe A, Geneston T, et al. An algorithm for diagnosis of proton exchange membrane fuel cells by electrochemical impedance spectroscopy. *Electrochim Acta* 2014;135:368–79. <https://doi.org/10.1016/j.electacta.2014.04.108>.
- [22] Kadyk T, Hanke-Rauschenbach R, Sundmacher K. Nonlinear frequency response analysis of PEM fuel cells for diagnosis of dehydration, flooding and CO-poisoning. *J Electroanal Chem* 2009;630:19–27. <https://doi.org/10.1016/j.jelechem.2009.02.001>.
- [23] Petrone R, Zheng Z, Hissel D, Péra MC, Yousfi-Steiner N. A review on model-based diagnosis methodologies for PEMFCs. *Int J Hydrogen Energy* 2013;38:7077–91. <https://doi.org/10.1016/j.ijhydene.2013.03.106>.
- [24] Kim J, Lee I, Tak Y, Cho BH. Impedance-based diagnosis of polymer electrolyte membrane fuel cell failures associated with a low frequency ripple current. *Renew Energy* 2013;51:302–9. <https://doi.org/10.1016/j.renene.2012.09.053>.
- [25] Giurgea S, Tirnovan R, Hissel D, Outbib R. An analysis of fluidic voltage statistical correlation for a diagnosis of PEM fuel cell flooding. *Int J Hydrogen Energy* 2013;38:4689–96. <https://doi.org/10.1016/j.ijhydene.2013.01.060>.
- [26] Legros B, Thivel P-X, Bultel Y, Nogueira RP. First results on PEMFC diagnosis by electrochemical noise. *Electrochem Commun* 2011;13(12):1514–6. <https://doi.org/10.1016/j.elecom.2011.10.007>.
- [27] Rubio M, Bethune K, Urquia A, St-Pierre J. Proton exchange membrane fuel cell failure mode early diagnosis with wavelet analysis of electrochemical noise. *Int J Hydrogen Energy* 2016;41:14991–5001. <https://doi.org/10.1016/j.ijhydene.2016.05.292>.
- [28] Damour C, Benne M, Grondin-Perez B, Bessafi M, Hissel D, Chabriet J-P. Polymer electrolyte membrane fuel cell fault diagnosis based on empirical mode decomposition. *J Power Sources* 2015;299:596–603. <https://doi.org/10.1016/j.jpowsour.2015.09.041>.
- [29] Benouioua D, Candusso D, Harel F, Oukhellou L. Fuel cell diagnosis method based on multifractal analysis of stack voltage signal. *Int J Hydrogen Energy* 2014;39:2236–45. <https://doi.org/10.1016/j.ijhydene.2013.11.066>.
- [30] Lee C-Y, Lee Y-M. In-situ diagnosis of local fuel cell performance using novel micro sensors. *Int J Hydrogen Energy* 2012;37:4448–56. <https://doi.org/10.1016/j.ijhydene.2011.11.098>.

- [31] Mohammadi A, Guilbert D, Gaillard A, Bouquain D, Khaburi D, Djerdir A. Faults diagnosis between PEM fuel cell and DC/DC converter using neural networks for automotive applications. In: IECON 2013-39th annual conference of the IEEE industrial electronics society. IEEE; 2013. p. 8186–91. <https://doi.org/10.1109/IECON.2013.6700503>.
- [32] Steiner NY, Hissel D, Mocotéguy P, Candusso D. Diagnosis of polymer electrolyte fuel cells failure modes (flooding & drying out) by neural networks modeling. *Int J Hydrogen Energy* 2011;36:3067–75. <https://doi.org/10.1016/j.ijhydene.2010.10.077>.
- [33] Shao M, Zhu X-J, Cao H-F, Shen H-F. An artificial neural network ensemble method for fault diagnosis of proton exchange membrane fuel cell system. *Energy* 2014;67:268–75. <https://doi.org/10.1016/j.energy.2014.01.079>.
- [34] Laribi S, Mammam K, Hamouda M, Sahli Y. Impedance model for diagnosis of water management in fuel cells using artificial neural networks methodology. *Int J Hydrogen Energy* 2016;41:17093–101. <https://doi.org/10.1016/j.ijhydene.2016.07.099>.
- [35] Liu J, Li Q, Chen W, Yan Y, Wang X. A fast fault diagnosis method of the PEMFC system based on extreme learning machine and Dempster-Shafer evidence theory. *IEEE Transactions on Transportation Electrification* 2018;5(1):271–84. <https://doi.org/10.1109/TTE.2018.2886153>.
- [36] Li Z, Outbib R, Hissel D, Giurgea S. Online diagnosis of PEMFC by analyzing individual cell voltages. 2013 European Control Conference (ECC). IEEE 2013:2439–44. <https://doi.org/10.23919/ECC.2013.6669725>.
- [37] Li Z, Giurgea S, Outbib R, Hissel D. Online diagnosis of PEMFC by combining support vector machine and fluidic model. *Fuel Cells* 2014;14:448–56. <https://doi.org/10.1002/fuce.201300197>.
- [38] Li Z, Outbib R, Giurgea S, Hissel D, Jemei S, Giraud A, et al. Online implementation of SVM based fault diagnosis strategy for PEMFC systems. *Appl Energy* 2016;164:284–93. <https://doi.org/10.1016/j.apenergy.2015.11.060>.
- [39] Li Z, Outbib R, Hissel D, Giurgea S. Diagnosis of PEMFC by using data-driven parity space strategy. In: European control conference (ECC). IEEE; 2014. p. 1268–73. <https://doi.org/10.1109/ECC.2014.6862527>. 2014.
- [40] Li Z, Cadet C, Outbib R. Diagnosis for PEMFC based on magnetic measurements and data-driven approach. *IEEE Trans Energy Convers* 2018;34:964–72. <https://doi.org/10.1109/TEC.2018.2872118>.
- [41] Mao L, Jackson L, Dunnett S. fault diagnosis of practical polymer electrolyte membrane (PEM) fuel cell system with data-driven approaches. *Fuel Cells* 2017;17(2):247–58. <https://doi.org/10.1002/fuce.201600139>.
- [42] Zheng Z, Petrone R, Péra MC, Hissel D, Becherif M, Pianese C, et al. A review on non-model based diagnosis methodologies for PEM fuel cell stacks and systems. *Int J Hydrogen Energy* 2013;38:8914–26. <https://doi.org/10.1016/j.ijhydene.2013.04.007>.
- [43] Jeppesen C, Araya SS, Sahlin SL, Thomas S, Andreasen SJ, Kær SK. Fault detection and isolation of high temperature proton exchange membrane fuel cell stack under the influence of degradation. *J Power Sources* 2017;359:37–47. <https://doi.org/10.1016/j.jpowsour.2017.05.021>.
- [44] Itoga M, Hamada S, Mizuno S, Nishiumi H, Murata K, Tonuma T. Development of fuel cell stack for new FCV. SAE Technical Paper; 2016. <https://doi.org/10.4271/2016-01-0529>.
- [45] Giri D, Acharya UR, Martis RJ, Sree SV, Lim T-C, VI TA, et al. Automated diagnosis of coronary artery disease affected patients using LDA, PCA, ICA and discrete wavelet transform. *Knowl Based Syst* 2013;37:274–82. <https://doi.org/10.1016/j.knosys.2012.08.011>.
- [46] Li Z, Outbib R, Hissel D, Giurgea S. Data-driven diagnosis of PEM fuel cell: a comparative study. *Contr Eng Pract* 2014;28:1–12. <https://doi.org/10.1016/j.conengprac.2014.02.019>.
- [47] Martínez AM, Kak AC. Pca versus lda. *IEEE Trans Pattern Anal Mach Intell* 2001;23:228–33. <https://doi.org/10.1109/34.908974>.
- [48] Ye J. Characterization of a family of algorithms for generalized discriminant analysis on undersampled problems. *J Mach Learn Res* 2005;6:483–502.
- [49] Tipping ME. Sparse Bayesian learning and the relevance vector machine. *J Mach Learn Res* 2001;1:211–44.
- [50] Li N, Liu C, He C, Li Y, Zha X. Gear fault detection based on adaptive wavelet packet feature extraction and relevance vector machine. *Proc Inst Mech Eng C J Mech Eng Sci* 2011;225:2727–38. <https://doi.org/10.1177/0954406211400691>.
- [51] Liu J, Yan Y, Li Q, Chen W. mRVM based fault diagnosis strategy for PEMFC systems of hybrid tramway. 2017 Chinese Automation Congress (CAC). IEEE; 2017. p. 1096–100. <https://doi.org/10.1109/CAC.2017.8242929>.
- [52] Widodo A, Kim EY, Son J-D, Yang B-S, Tan AC, Gu D-S, et al. Fault diagnosis of low speed bearing based on relevance vector machine and support vector machine. *Expert Syst Appl* 2009;36:7252–61. <https://doi.org/10.1016/j.eswa.2008.09.033>.
- [53] Zhang C, He Y, Yuan L, Deng F. A novel approach for analog circuit fault prognostics based on improved RVM. *J Electron Test* 2014;30:343–56. <https://doi.org/10.1007/s10836-014-5454-8>.
- [54] Liu J, Li Q, Chen W, Yan Y, Qiu Y, Cao T. Remaining useful life prediction of PEMFC based on long short-term memory recurrent neural networks. *Int J Hydrogen Energy* 2019;44:5470–80. <https://doi.org/10.1016/j.ijhydene.2018.10.042>.
- [55] Li Z, Outbib R, Giurgea S, Hissel D, Giraud A, Couderc P. Fault diagnosis for fuel cell systems: a data-driven approach using high-precise voltage sensors. *Renew Energy* 2019;135:1435–44. <https://doi.org/10.1016/j.renene.2018.09.077>.
- [56] Li Z, Outbib R, Hissel D, Giurgea S. Diagnosis for PEMFC systems : a data-driven approach with the capabilities of online adaptation and novel fault detection. *IEEE Trans Ind Electron* 2015;62:5164–74. <https://doi.org/10.1109/TIE.2015.2418324>.